Carbonation of brine impacted fractionated coal fly ash: Implications for CO2 sequestration

Muriithi Grace Nyambura [a, *], Gitari Wilson Mugera [b], Petrik Leslie Felicia [a], Ndungu Patrick Gathura [a]

[a] Environmental and Nano Sciences Group, Department of Chemistry, University of the Western Cape, Private Bag X17, Bellville, 7535, Cape Town, South Africa

[b] Department of Ecology and Resource Management, School of Environmental studies, University of Venda. Private bag, X5050, Thohoyandou, 0950, Limpopo, South Africa

* Corresponding author. Tel./fax: þ27 21 9593878.
E-mail address: gmuriithi@uwc.ac.za (M.G. Nyambura).

Abstract

Coal combustion by-products such as fly ash (FA), brine and CO2 from coal fired power plants have the potential to impact negatively on the environment. FA and brine can contaminate the soil, surface and ground water through leaching of toxic elements present in their matrices while CO2 has been identified as a green house gas that contributes significantly towards the global warming effect. Reaction of CO2 with FA/brine slurry can potentially provide a viable route for CO2 sequestration via formation of mineral carbonates. Fractionated FA has varying amounts of CaO which not only increases the brine pH but can also be converted into an environmentally benign calcite. Carbonation efficiency of fractionated and brine impacted FA was investigated in this study. Controlled carbonation reactions were carried out in a reactor set-up to evaluate the effect of fractionation on the carbonation efficiency of FA. Chemical and mineralogical characteristics of fresh and carbonated ash were evaluated using XRF, SEM, and XRD. Brine effluents were characterized using ICP-MS and IC. A factorial experimental approach was employed in testing the variables. The 20e150 mm size fraction was observed to have the highest CO2 sequestration potential of 71.84 kg of CO2 per ton of FA while the >150 mm particles had the lowest potential of 36.47 kg of CO2 per ton of FA. Carbonation using brine resulted in higher degree of calcite formation compared to the ultra-pure water carbonated residues.

Keywords: Fly ash, Brine, CO2 sequestration, Carbonation efficiency

1. Introduction

Coal combustion provides 40% of the world's energy needs; nevertheless this figure is projected to increase due to the increasing demand for electricity and the availability of large coal reserves in different parts of the world. However, coal combustion leads to emission of environmentally harmful gases such as CO2, SO_X, NO_X, and chlorofluorocarbons (CFC) and ozone (O3). CO2 whose atmospheric concentration has

risen from pre-industrial levels of 280 ppm to 380 ppm in 2005 (Bachu, 2008) is the most important green house gas (GHG), being responsible for about two-thirds of the enhanced green house effect. Currently, China's CO_2 emissions surpass those of the USA by 8%. South Africa on the other hand generates 93% of its electricity from coal combustion with CO_2 emissions of over 218 Mt annually (Engelbrecht et al., 2004). Despite the numerous environ- mental issues associated with its combustion, coal will remain a major source of electric power in South Africa for years to come owing to the relative lack of suitable alternatives to coal as an energy source coupled with the large coal deposits which can be exploited at extremely favorable costs (Randall, 2002). It thus follows that a major advance in tackling global warming could be achieved by curtailing atmospheric emissions of CO_2 from coal fired power plants.

Other coal combustion by-products (CUB) such as fly ash (FA), bottom ash, slag and flue gas desulphurization (FGD) products are formed from the non-combustible portion of the coal. Of the one billion metric tons of coal mined annually in the USA, about 90% is burned to generate electricity with a production of over 100 million tons of CUB annually (Kutchuko and Kim, 2006). Over 36.4 Mt of FA are produced by the electricity production industry in South Africa per annum with only about 5% of it being utilized while the remaining is disposed in ash dumps (Kruger, 2003). FA is enriched with a suite of trace elements such as V, Hg, Fe, Ba, B, Ca, Mg, K, Th, etc. Furthermore, the particle size ranges between 0.5 and 200 mm, thus FA is prone to leaching in the event of water percolation.

Waste brine streams produced in power plants from pre-treatment of raw water for boiler feed through processes such as reverse osmosis (RO) and electro reversal dialysis (EDR) are loaded with Na, Cl, SO_4, Ca, Mg and a host of trace elements such as Fe, Mn, Cr, V, Ti, P, Si and Al. The main environmental concern with respect to the disposal of FA and brine is the release of inorganic contaminants including soluble salts and trace metals as a result of leaching processes (Baciocchi et al., 2009). It is imperative that proper management of these three "wastes stream", i.e. CO_2, FA and brine is devised so as to continue exploitation of natural resources like coal in an environmentally sustainable manner.

The existing methods available for the carbon sequestration process include adsorption by physical and chemical wet scrubbing, adsorption by solids using pressure and temperature swing modes, cryogenic distillation and mineral carbonation (Yadav et al., 2009). Mineral carbonation is an attractive alternative method for the removal of carbon dioxide as it results in permanent storage of carbon dioxide as mineral carbonates that are environmentally benign and which can be used for mine backfilling (Yadav et al., 2009). As has been shown previously (Soong et al., 2006; Druckenmiller and Maroto-Valer, 2005) carbonation of coal FA and brine has the capacity to sequester CO_2 in the form of carbonates. However there is no data available on the carbonation efficiency of brine impacted and size fractionated South African FA. The objective of this study is to correlate the carbonation efficiency between different size fractions of Class F, South African FA.

This study is especially attractive since the residual solid and liquid by- products from power plants could be used to mitigate the residual gaseous wastes produced by the same plants.

2. Material and methods

The FA and brine samples used in this study were collected from coal burning power plants in the Mpumalanga province of South Africa. Fractionation was achieved by use of an Endecott mechanical shaker. Morphological analysis was done by Scanning Electron Microscopy (Hitachi X-650 scanning Electron Microanalyser equipped with a CDU- lead detector at 25 mkV). Crystalline phases present in the FA were determined by X-Ray Diffraction Spectroscopy (XRD) using a Bruker AXSD8 Advance diffractometer coupled with a Cu-Ka radiation at 40 kV and 40 mA with a PSD Lynx-Eye, Sistrip detector at 0.03 deg/step 2 theta from 12° to 80° and 3 scounting time. Elemental analysis of FA was done by XRF using a Philips PW 1480 X-ray spectrometer fitted with a Cr tube and five analyzing crystals namely LIF 200, LIF 220, GE, PE and PX at 40 kV and 50 mA tube operating conditions. Chittick tests were carried out to determine the % $CaCO_3$ in the carbonated FA by reacting 1.70 g of the carbonated FA with 20 ml of 6 N HCl and recording the amount of CO_2 evolved by reading the displacement of the reservoir fluid. TGA/DSC was carried out using a Mettler Toledo TGA/SDTA 851e with sample robot and a TSO800 GC gas control unit. Anions present in the brine as well as the carbonation leachates were analyzed with an Ion Pac AS14A column and AG14-4 mm guard column. Major cations were analyzed using a Varian radial ICP-AES while trace cations were done on an Agilent 7500ce ICP-MS using.High Matrix Introduction (HMI) accessory and He as collision gas.

2.1. Carbonation procedure

The carbonation reactions were carried out in a stainless steel autoclave reactor with a 600 ml volume capacity. The brine and FA slurry were contained in a teflon liner which was placed inside a steel jacket. A schematic of the reactor is shown in Fig. 1

Two different temperatures of carbonation were used (30 ^{O}C and 90 ^{O}C) while the pressure of CO_2 was varied between 1 MPa and 4 MPa. To investigate the influence of solid/liquid (S/L) ratio on carbonation, S/L ratios were varied between 0.1, 0.5 and 1. The size fractions of FA used were <20 mm, 20e150 mm, >150 mm and bulk ash. The dispersion (brine þFA at the required S/L ratio) was placed inside the teflon liner in the pressure vessel and closed. Following the sealing of the pressure vessel, the body of the reactor was placed in the heater assembly and the thermocouple, magnetic stirrer drive system, and water coolant supply controlled by a solenoid valve were put in place. The gas supply connection for the CO_2 (Afrox, technical grade) feed line was then attached. The system was then purged three times with CO_2 at 0.05 MPa to ensure that all the air was expelled after which the heating system was switched on.

When the specified temperature was reached, CO_2 was charged into the reactor to achieve the specified reaction pressure. The brine/FA/CO_2 mixture was then stirred at 600 rpm for 2 h to prevent any settling of solids during the experiments. At the end of the experiment, the reactor was removed from the heating system and was quenched in cold water. The reaction cell was depressurized for 15 min during the water cooling period. Upon cooling to room temperature, the reactor was disassembled, and the solid product was separated by centrifugation (30 min at 6000 rpm), thereafter the supernatant solutions were decanted. Finally, the solid product was dried in a vacuum oven for 8 h at 90 °C and analysed by XRD and Chittick test. The supernatant solutions were filtered through a 0.2 mm pore membrane. The filtered solutions for cation analysis were immediately acidified to pH <2 while those for anion analysis were stored as they were, i.e., without acidification. The samples were refrigerated at 4 °C until analysis.

3. Results and discussions

3.1. Chemical analysis by X-ray fluorescence

The fractionated and un-carbonated FA was characterized chemically using XRF in order to quantify the present major, minor and trace elements. Table 1 below gives the results for the major and minor elements while the trace elements partitioning is given in Fig. 2.

Fresh South African FA contains SiO_2, Al_2O_3, Fe_2O_3 and CaO as the major oxides. The ash can therefore be classified as Class F since the sum of the percentage composition of SiO_2, Al_2O_3 and Fe_2O_3 is greater than 70% according to the American Society for Testing and Materials (1993). Furthermore, the CaO content is lower than 10%
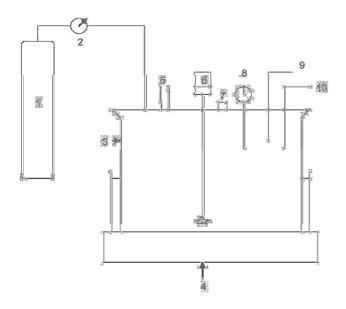
Fig. 1. Schematic of the reactor. (1) Carbon dioxide cylinder. (2) Pressure regulator. (3) Stainless steel reactor vessel (maximum temperature = 350 °C with teflon liner, maximum pressure = 345 bar). (4) Heating jacket. (5) Pressure relief valve. (6) Stirrer powered by a magnetic drive. (7) Thermocouple. (8) Pressure gauge. (9) Liquid sampling point.

Table 1
Major elements concentration (bulk and fractionated un-carbonated ash).

Majors (wt %)	Bulk	>150 mm	150e106 mm	106e90 mm	90e75 mm	75e63 mm	63e53 mm	53e45 mm	45e32 mm	32e25 mm	25e20 mm	<20 mm
SiO_2	51.227	42.458	50.640	51.770	52.417	52.668	51.400	52.641	52.373	52.709	52.761	51.1181

TiO2	1.548	0.979	1.214	1.333	1.514	1.580	1.616	1.630	1.655	1.684	1.695	1.844
Al2O3	26.000	17.968	22.034	24.055	25.270	25.979	27.224	26.355	27.352	26.554	27.353	28.510
Fe2O3	2.430	1.984	3.472	2.628	2.756	2.426	2.419	2.280	2.394	2.243	2.245	2.572
MnO	0.061	0.041	0.058	0.062	0.064	0.062	0.063	0.062	0.059	0.065	0.061	0.064
MgO	2.439	1.662	2.342	2.513	2.714	2.534	2.569	2.451	2.499	2.480	2.472	2.624
CaO	9.198	5.894	9.014	9.671	10.286	9.484	9.591	9.261	9.129	8.768	8.498	8.634
Na2O	0.457	0.146	0.281	0.287	0.355	0.385	0.384	0.466	0.537	0.582	0.558	0.688
K2O	0.787	0.652	0.778	0.746	0.768	0.778	0.781	0.796	0.815	0.823	0.823	0.872
P2O5	0.698	0.438	0.542	0.576	0.691	0.718	0.747	0.755	0.770	0.781	0.777	0.878
SO3	0.35	0.360	0.26	0.26	0.301	0.351	0.317	0.368	0.375	0.379	0.385	0.395
Cr2O3	0.033	0.022	0.029	0.031	0.033	0.034	0.036	0.040	0.038	0.040	0.041	0.041

which is also a grading criterion for Class F FA. CaO in FA is present as free lime and embedded in glassy spheres. Usually the CaO content increases with decreasing particle size. However, the content can also decrease due to formation of glassy spheres from free lime and alumino silicate melt or the reaction of free lime with SO_2 via $CaSO_3$ to anhydrite (Enders, 1996). Bearing in mind that the amorphous glassy spheres are the most important Al_2O_3 bearing phases, Al_2O_3 content of size fractions is an indicator of the amount of amorphous glass in FA (Enders, 1996). An increasing trend with decreasing particle size is clearly visible for Al_2O_3 while the 75e90 mm fraction had the highest lime content.

In the un-carbonated ash, S, Sr, Ba, Zr, Mn, Cr and V are the main traces present with levels above 100 ppm, though an increasing trend is observed with decreasing particle size for Cu, Ni, Zn, Ba, Zr, Cr and V. Mn showed a constant trend throughout the chosen particle size range. It is also evident that the bulk ash had lower concentrations of all the trace elements unlike the smaller size fractions. Based on the degree of concentration dependence on particle size, the elements can be categorized into three groups namely (a) elements showing a pronounced trend of increased concentration with decreasing particle size, i.e. Cu, Ni, Zn, Ba, Zr, Cr and V in fresh ash. (b) Elements showing limited concentration trends, i.e. Sr, S, Y, Th, Nb, Rb and Pb (c) those elements showing no concentration trends, i.e. Mn in fresh FA. Elements showing greatest concentration dependence with particle size are generally associated with elemental forms that boil or sublime at coal combustion temperatures. Fine particles with their large ratio of surface area to mass preferentially concentrate these elements (Sarkar et al., 2006). Several studies have

noted that the most salient features of FA are the gradation effects of particle size on elemental concentration (Klein et al., 1995; Kaakinen et al., 1975; Davison et al., 1974).

It can be concluded that the smaller the FA particle size, the more leachable toxic trace elements present. Furthermore these particles are expected to be more reactive due to the high surface area to volume ratio. This would mean that the traces species therein are more bio-available and thus prone to leaching in case of water percolation which could in turn lead to surface and ground water contamination.

3.2 Brine analysis and classification

The brine utilized for carbonation was obtained from the RO circuit of a coal combustion power plant in Mpumalanga. Table 2 gives the analysis of the various ions present in the brine while the classification is shown in Fig. 3 below. The brine solutions can be classified as $NaSO_4$ water as these are the main ions present. Other significant ions include Ca, K, Mg and Cl with trace quantities of NO_3, PO_4, Al, As, Ba, Cd, Co, Cr, Cu, Fe, Mn, Mo, Ni, Pb, Se, Sr, V and Zn. This has been reported elsewhere (Petrik et al., 2007).

3.3 Morphological analysis by scanning electron microscopy

The morphology of un-carbonated and carbonated FA was evaluated by SEM and the difference in the structure of the FA particles before and after carbonation could be observed in Fig. 4. Micrographs of fresh un-carbonated South African FA show the presence of spherical particles (Fig. 4a), cenospheres (Fig. 4a) and plerospheres (Fig. 4b). The fine fraction of FA particles are typically well-rounded, solid spheres and the larger particles within the larger size fraction samples contain a few particles up to 0.5 mm with cenospheres common and an occasional plerosphere. Some of the larger particles are vesicular (i.e. made up of small spherical or oval cavity produced by the presence of bubbles of gas or vapour). Pieterson (1993) attributes the origin of the vesicles to generation of gases and vapors such as CO, CO_2, SO_2 and H_2O giving FA its light weight characteristics. The carbonated FA however shows "cubic-like" structure of calcite (Fig. 4c); while in Fig. 4d "needle-like" structures of aragonite are observed. Similar morphologies of carbonated FA have been reported (Perez-Lopez et al., 2008; Montes-Hernandez et al., 2009; Fernandez et al., 2004), where calcite was identified as the main polymorph of $CaCO_3$ formed during the carbonation process.
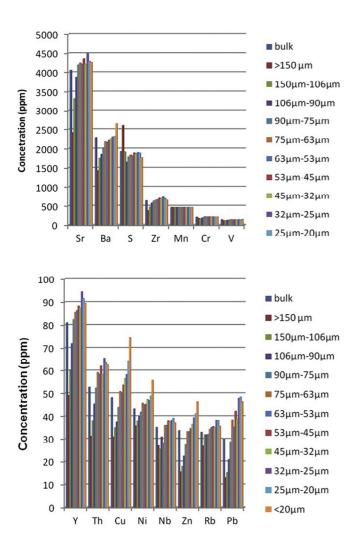
Fig. 2. Trace elements concentration in un-carbonated FA.

Table 2
Brine solution concentrations.

Species	RO brine (ppm)
K	104.1 ± 0.31
Al	0.044 ± 0.06
As	0.007
Ca	101.76 ± 0.15
Co	0.015 ± 0.01
Cr	0.014 ± 0.01
Cu	0.067 ± 0.02
Fe	0.051 ± 0.01
Mg	158.73 ± 1.24
Mn	0.082 ± 0.03
Mo	0.039 ± 0.01
Na	4315 ± 2.18
Ni	0.116 ± 0.01
Se	0.004
Sr	3.030 ± 0.11
V	0.016 ± 0.01
Zn	0.100 ± 0.01
Cl	2036 ± 3.26
SO_4	9488 ± 2.22
NO_3	8.565 ± 0.61

3.4. X-Ray diffraction analysis of fresh ash and carbonated ash

The diffraction pattern of the fresh un-carbonated ash as well as the carbonated ash are shown in Figs. 5 and 6.

The CaO fraction present in the pre-carbonated ash (Fig. 5) is converted to calcite in the post-carbonated ash. Presence of calcite peak can be observed (Fig. 6) thus XRD confirmed the conversion of CaO to calcite during the carbonation process confirming the observations made from the SEM morphology of the carbonated ash.

3.5. Comparative study of the formed calcium carbonate

Fig. 7 shows the correlation of the mass % $CaCO_3$ yield as determined by quantitative XRD and Chittick tests. The two methods were applied in quantifying the mass % of $CaCO_3$ formed in the carbonation process.
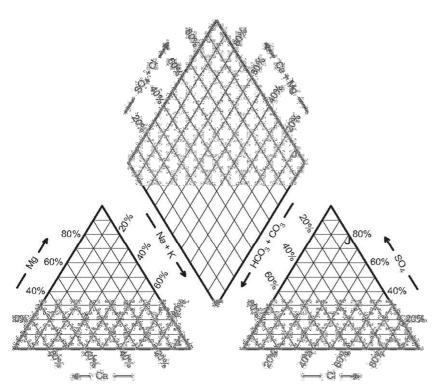
As is evident from Fig. 7, the mass % of CaCO3 could be determined by both methods as a strong correlation was observed except for runs R2, R14, R24, R25, R27 and R29. Statistical testing was carried out to determine whether Chittick tests gave a better estimate of the % CaCO3 than XRD. Student t-test statistic was applied to test the hypothesis that Chittick test gave a higher overall % CaCO3 yield than XRD.

$$t = \frac{\mu_1 - \mu}{\sqrt{\frac{\sum d^2 - \frac{(\sum d)^2}{N}}{N(N-1)}}}$$ (1)

where m_1 and m_2 are the means of the two data sets (m_1 is the mean of X_1 and m_2 is the mean of X_2), d is the difference between the two data sets and N is the sample size. Table 3 gives the data applied in the t-test formula.

The calculated value of t of 2.198 was greater than the tabulated value of 1.701. The null hypothesis was thus rejected and it was concluded that Chittick analysis gave a higher overall % $CaCO_3$ yield.

Further, a measure of agreement or concordance by using the concordance correlation coefficient was also tested as described by Lin (1989). The concordance correlation coefficient is a measure of scatter of the data points around the identity line (the X ¼ Y line).

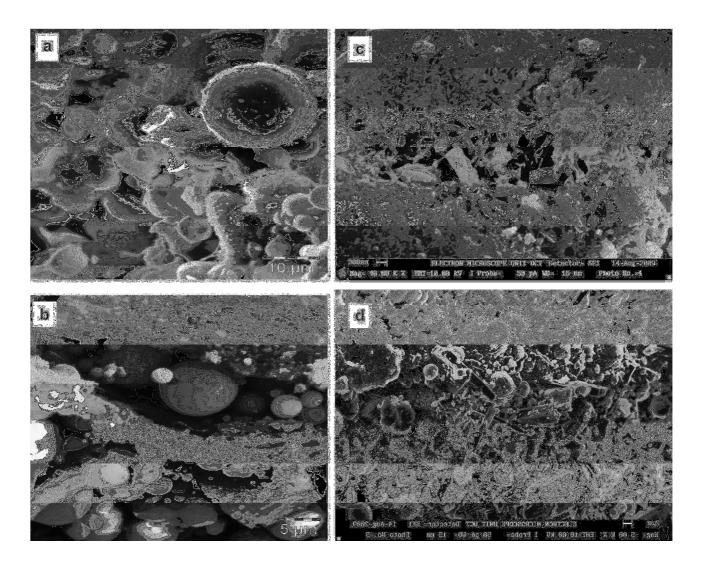Fig. 3, Piper diagram for brine classification.

Fig. 4. SEM micrographs showing un-carbonated (a & b) and carbonated (c &d) FA.

The following statistics were obtained using SAS statistical program in testing for the concordance correlation coefficient (Table 4).

In the analysis of concordance correlation coefficient, Chittick test was set as test 1 and XRD as test 2. Thus n1 and n2 are the sample sizes for Chittick and XRD; N is the average sample size, mean 1 and mean 2 give the values of the means for both Chittick test and XRD. The Pearson correlation coefficient which is obtained by dividing the covariance of the two methods with the products of their standard deviations gave a value of 0.799 which is indicative of a relatively high degree of correlation. The concordance correlation coefficient is essentially supposed to be 1 for high correlation and the value of 0.682 obtained in this study means that most of the points are relatively far from the identity line (where X ¼ Y in this case the line is 2, 2e7, 7) when the values from Chittick test are plotted against those of XRD as shown in Fig. 8.

From Fig. 8, one notices that majority of the points lie above the identity line which means that test 1 (Chittick test in this case) gives higher values for the % $CaCO_3$ yield, further confirming the observations from the t-test.
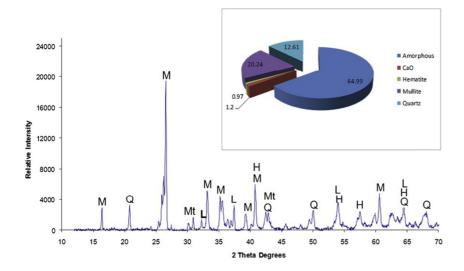
Fig. 5. Phase identification and quantification of fresh FA by XRD; M (mullite), Q (quartz), Mt (magnetite), L(lime), H (hematite).

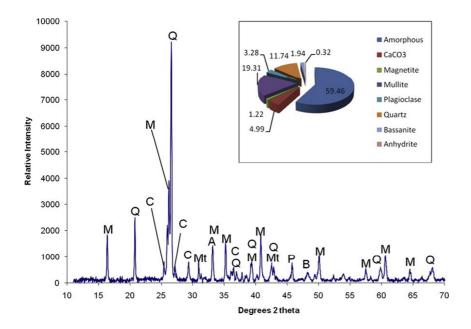Fig. 6. Phase identification and quantification for carbonated FA by XRD; (90 ⁰ C, 4 MPa, bulk ash at an S/L ratio of 1); M (mullite), Q (quartz), C (calcite), A (anhydrite), P (plagioclase), B (bassanite), Mt (magnetite).

3.6. Carbonation efficiency of the fractionated South African FA

For pure oxides (e.g. CaO and Ca(OH)2), the theoretical extent of carbonation is a function of basic stoichiometry (Huntzinger et al., 2009):

$$CaO_{(s)} + CO_{2(aq)} \rightarrow CaCO_{3(s)} \qquad (2)$$

Using the simple equation of mass ¼ moles x molar mass, and bearing in mind that the molar ratio is 1:1, it follows that every ton of CaO can potentially sequester up to 799 kg of CO_2. For wastes such as FA, the theoretical extent of carbonation can also be calculated as a function of stoichiometry, though in this case the extent of carbonation will also depend on the availability of the oxides for reaction. Theoretically the maximum CO_2 uptake capacity can be calculated as a function of the chemical composition of the original material (i.e. FA) using the Stenoir formula (Fernandez et al., 2004):

$$CO_2\ (\%) = 0.785\ (\%\ CaO - 0.7\%\ SO_3) + 1.09\%\ Na_2O + 0.93\%\ K_2O \qquad (3)$$

The stoichiometric mass factors shown in Eq. (3) assume that all of the CaO (except that bound in $CaSO_4$ and $CaCO_3$) will react to form $CaCO_3$, all the MgO will react to form $MgCO_3$, and all of Na_2O and K_2O will convert to Na_2CO_3 and K_2CO_3. The mass factors for K_2O and Na_2O are doubled if bicarbonates form instead of carbonates (Huntzinger et al., 2009). Furthermore the degree of carbonation is strongly dependent upon calcium content, though the presence of certain components might influence the effective diffusivity and reactivity of the CO_2 (Fernandez et al., 2004).
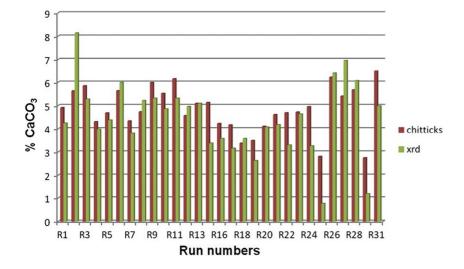

Fig. 7. Correlation of mass % $CaCO_3$ yield determined by quantitative XRD and Chittick test.

Table 3
Data for student t-test of quantitative XRD and Chittick test.

Run no.	Chittick test (X_1)	XRD (X_2)	Difference (d)	Squared d (d^2)
R1	4.92	4.25	0.67	0.45
R2	5.64	8.14	−2.5	6.25
R3	5.86	5.28	0.52	0.39
R4	4.31	3.39	0.52	0.30
R5	4.68	4.98	0.51	0.20
R6	5.64	76	−1.96	0.36
R7	4.29	3.4	0.52	0.22
R8	4.39	5.25	−0.48	0.72
R9	6.00	5.32	0.68	0.46
R10	5.52	4.86	0.66	0.44
R11	6.16	5.32	0.84	0.71
R12	4.57	4.96	−0.39	0.15
R13	5.10	5.1	0	0
R14	5.14	3.38	1.76	3.10
R16	4.23	3.58	0.65	0.42
R17	4.17	3.16	1.01	1.02
R18	3.38	3.58	−0.2	0.04
R19	3.50	2.63	0.87	0.76
R20	4.11	4.08	0.03	0
R21	4.62	4.18	0.44	0.19
R22	4.69	3.3	1.39	1.93
R23	4.73	4.64	0.09	0.01
R24	4.96	3.26	1.7	2.89
R25	2.81	0.77	2.04	4.16
R26	6.22	6.4	−0.18	0.03
R27	5.41	6.96	−1.55	2.40
R28	5.68	6.07	−0.39	0.15
R29	2.75	1.21	1.54	2.37
R31	6.50	4.99	1.51	2.28
$N = 29$	$\mu_1 = 4.84$	$\mu_2 = 4.44$	$\Sigma d = 11.57$ $(\Sigma d)^2 = 133.86$	$\Sigma d^2 = 31.38$

Using Eq. (3) and the data in Table 1 for the different oxides present in the different partitions of the fresh FA, the maximum % CO_2 uptake for all the FA size fractions can thus be calculated as follows.

From Table 5, it means that theoretically, assuming all available oxides react to form carbonates, the sequestration capacity of bulk fly ash for instance is 8.2537%, i.e. for every 1 ton of bulk FA, 82.54 kg of CO_2 can be sequestered. Bearing in mind that the 20e150 mm fraction was combined as one and its average CaO was 9.3 g the % CO_2 uptake would theoretically amount to 8.3148% meaning that the for every ton of 20e150 mm fraction, 83.15 kg of CO_2 could be sequestered. It is thus clear that the higher the lime content of a fraction the higher the sequestration capacity of that fraction. On the other hand the >150 mm fraction which had the lowest lime content (as observed in Table 1) gave the lowest theoretical % CO_2 showing that its sequestration capacity is the lowest.

CaO in the FA is the main source of the Ca^{2+} though the Ca^{2+} in brine also contributes towards the total Ca cations available for carbonation. Fernandez et al. (2004) evaluated the effect of particle size in carbonation of municipal solid waste incinerator (MSWI) ash and observed that carbonation was higher with smaller particles sizes. They attributed this observation to the higher CaO content of the smaller particle sizes, homogeneity of the particle sizes as well as the higher surface area of these particles.

Knowing the pressure drop due to carbonation, the amount of CO_2 consumed by carbonate precipitation can be calculated using the ideal gas law (Perez-Lopez et al., 2008; Montes-Hernandez et al., 2009) as follows:

Table 4
Concordance correlation coefficient data.

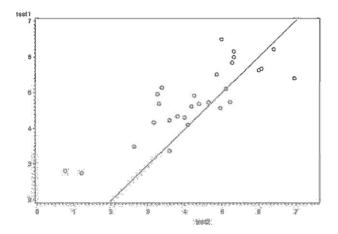| n1	n2	N	Mean 1	Mean 2	Std 1	Std 2	Pearson	Concordance correlation
29	29	29	4.84	4.44	0.95	1.53	0.799	0.682
		Concordance Corr Lower 95% CI	Concordance Corr Upper 95% CI		Location shift		Scale shift	correction
	0.497	0.808	0.231		0.621			0.854

Fig. 8. Plot of the concordance correlation coefficient for Chittick test and XRD (test 1 is Chittick test while test 2 is XRD).

$$nCO_2 = \frac{P_{carbonation\_pressure\_drop}V}{RT} \quad (4)$$

where V is the reactor volume occupied with gas. The teflon liner used together with the steel jacket was not a tight fit and hence the volume of gas in this study was, the volume of the steel jacket minus volume of the teflon liner minus the volume occupied by the solid and liquid mixture in the teflon. The teflon volume was calculated by a simple displacement experiment where the volume displaced by the teflon was taken to be its volume (observed to be 200 cm^3). The volume of the steel jacket was calculated from the equation for the volume of a cylinder i.e. $V = \pi r^2 h$, (r = radius of the jacket (3.15 cm), h = height of the steel jacket (15 cm) which gave a value of 467.65 cm^3). V was calculated for each run and the data used to calculate nCO_2 values for the runs. After the calculation of nCO_2, the carbonation efficiency of each run was calculated using Eq. (5) (Perez-Lopez et al., 2008; Montes-Hernandez et al., 2009):

$$CE = \frac{nCO_2 \times MCO_2}{\frac{WCaO}{MCaO} \times MCO_2} \times 100 \quad (5)$$

where nCO_2 is the number of moles consumed, calculated by Eq. (4) above, MCO_2 is the molar mass of CO_2 (44.01 g/mol), WCaO is the starting mass of the CaO in the

reactor (the corresponding amount of CaO in the size fraction in grams as seen in Table 1) and M_{CaO} is the molar mass of CaO (56.077 g/mol).

Applying Eq. (5) above and the information given in Table 6, the carbonation efficiency of fractionated FA was calculated, bearing in mind the conditions for each run. From Table 5, it can be seen that

Table 5
Maximum % CO$_2$ uptake for different size fractions.

Particle size	% CO$_2$
Bulk ash	8.2537
>150 μm	5.1668
150–106 μm	7.9624
106–90 μm	8.4533
90–75 μm	9.0103
75–63 μm	8.3953
63–53 μm	8.4996
53–45 μm	8.3014
45–32 μm	8.3035
32–25 μm	8.0744
25–20 μm	7.8330
<20 μm	8.1215

theoretically one ton of the 20e150 mm fraction can sequester 83.15 kg of CO$_2$. Bearing in mind the CE of this fraction it follows that a ton of this particle size range will actually sequester 71.8 kg of CO$_2$. It is evident (Table 6) that the input factors of pressure, temperature and particle size vary across the table. Overall, high pressure of 4 Mpa was necessary while both the temperatures (30 °C and 90 °C) gave high carbonation efficiency values.

The sequestration potential was calculated for the highlighted runs (i.e. runs 5, 10, 14, 20, 28 and 31) and the sequestration potentials per tonnage of fly ash are shown in Fig. 9 below based on the different size fractions applied.

It can be concluded that based on particle size, the fraction with the highest CO$_2$ sequestration potential is the 20e150 mm while the least potent is the >150 mm fraction. Montes-Hernandez et al. (2009) in their study on the carbonation of non-fractionated FA obtained a carbonation efficiency of 82% after 18 hours of carbonation at 30 °C. However the sequestration potential of their ash was lower, i.e. 26.19 kg of CO$_2$ per ton of FA as opposed to the value of 62.35 kg of CO$_2$ per ton of bulk FA observed in this study. This is attributable to two factors, firstly, the fractionated FA used in this study (Table 1) had a higher CaO content as opposed to theirs with a value of 4.1% of CaO and secondly, they used water for the carbonation experiments whereas brine was used in this study. This confirms that brine contributes additional Ca^{2+} for the carbonation process.

3.7. Comparisons of ultra-pure water and brine as the FA dispersion media in the carbonation experiments

Carbonation was also carried out for Run R31 with ultra-pure water (at 4 MPa, 90 °C, using bulk ash at an S/L ratio of 1) to compare the results with the findings

from Montes-Hernandez et al. (2009) and to determine the significance of using brine in place of ultra-pure water. Table 7 gives a comparison of the aqueous extract (leachate) recovered after carbonation using either ultra-pure water or RO brine solutions.
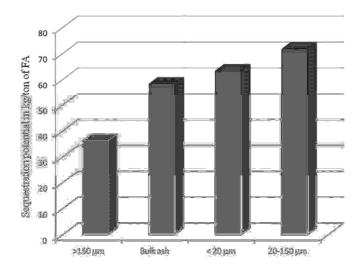

Fig. 9. Sequestration potential of the different size fractions.

The observation of lower concentrations of the various elements in the brine carbonated leachates can be attributed to the co- precipitation of the brine components with $CaCO_3$ as was suggested by Mooketsi et al. (2007). Table 7 shows that majority of the trace elements have a higher concentration in the water leachates than in the brine leachates except for Na. The Na content of the brine leachates is very high (3201 ppm) compared to the water leachates (58.05 ppm). From brine classification given in Fig. 3, it had been noted that the brine used were $NaSO_4$ rich solutions hence the high Na content for the brine leachate compared to the Na content of the water/FA leachates. The magnesium content of the water leachates is higher than that for the brine leachates, 103.24 ppm and 1.522 ppm, respectively. This signifies that Mg in brine takes part in the carbonation, though magnesite was not identified using XRD, maybe due to very low quantities being formed.

Table 6
Carbonation efficiencies (CE) for the various experimental runs.

Run no.	Temperature (^{0}C)	Pressure (Mpa)	Particle size (mm)	S/L ratio (g/ml)	Initial pressure (Mpa)	Final pressure	Pressure drop due to	nCO$_2$	CE (%)
1	90	1	<20	0.5	1	0.48	0.52	0.0203	13.2
2	90	1	20e150	0.5	1	0	1	0.0390	24.197
3	90	4	Bulk	0.1	4	0.55	3.45	0.01714	10.4
4	30	1	<20	0.5	1	0.55	0.45	0.0200	12.9
5	90	4	>150	0.5	4	1.03	2.97	0.07419	70.
6	90	1	20e15	1	1	0.14	0.86	0.0198	11.9
7	90	1	>150	0.1	1	0.17	0.83	0.00412	3.925
8	30	1	20e15	0.1	1	0.48	0.52	0.0030	1.87
9	90	4	20e15	0.1	4	0.76	3.24	0.01610	9.71
10	30	4	Bulk	0.5	4	1.52	2.48	0.11616	70.
11	90	4	20e15	0.1	4	0.69	3.31	0.01645	9.92
12	30	1	Bulk	0.1	1	0.34	0.66	0.0039	2.4
13	30	4	20e15	1	4	1.24	2.76	0.07636	46.
14	90	4	<20	1	4	0.59	3.41	0.12032	78.1
16	30	1	Bulk	1	1	0.28	0.72	0.01992	12.1
17	30	1	<20	0.5	1	0	1	0.0299	19.4
18	30	1	<20	0.1	1	0.07	0.93	0.00553	3.6
19	30	1	>150	0.5	1	0.31	0.69	0.03231	30.
20	30	4	Bulk	1	4	0.34	3.66	0.10126	61.7
21	90	4	<20	0.5	4	0.83	3.17	0.12393	80.
22	30	4	<20	1	4	0.21	3.79	0.10485	68.1
23	30	1	Bulk	0.5	1	0	1	0.0468	28.
24	90	4	<20	0.1	4	0.38	3.62	0.01799	11.6
25	30	4	>150	0.1	4	0.14	3.86	0.0229	21.8
26	90	1	20e15	0.1	1	0.07	0.93	0.0046	2.79
27	90	1	Bulk	0.5	1	0.07	0.93	0.03636	22.1
28	30	4	20e15	0.5	4	0.14	3.06	0.1433	86.
29	30	1	>150	0.1	1	0.14	0.86	0.00512	4.87
31	90	4	Bulk	1	4	0.83	3.17	0.11185	68.

Table 7
Concentrations of the raw brine, leachates obtained after carbonation using brine or ultra-pure water.

Element	Raw brine (ppm)	Run 31 (ultrawater) (ppm)	Run 31 (brine) (ppm)
K	1041 ± 0.31	23.5?? ± 1.3?	9.75 ± 0.17
Al	0.044 ± 0.07	0.053 ± 0.01	Nd
As	0.007	0.003	Nd
B	NA	2.08? ± 0.18	2.72? ± 0.0?
Ca	10176 ± 0.16	26651 ± 1.12	255 ± 1.02
Co	0.015 ± 0.001	Nd	0.002
Cr	0.014 ± 0.01	0.010	0.001
Cu	0.067 ± 0.02	0.044 ± 0.01	Nd
Fe	0.051 ± 0.01	0.030	Nd
Mg	158.73 ± 1.24	103.238 ± 2.01	1.522 ± 0.02
Mn	0.082 ± 0.03	Nd	Nd
Mo	0.039 ± 0.01	1.204 ± 0.03	0.069 ± 0.01
Na	4315 ± 2.18	58.048 ± 0.09	3201 ± 1.92
Ni	0.116 ± 0.01	0.112 ± 0.01	Nd
Se	0.004	0.094 ± 0.01	Nd
Sr	3.030 ± 0.11	2.019 ± 0.12	Nd
V	0.016 ± 0.01	4.559 ± 0.81	0.15 ± 0.01
Zn	0.100 ± 0.01	0.140 ± 0.01	Nd
Cl	2036 ± 3.26	Nd	2193 ± 2.03
SO_4	9488 ± 2.22	Nd	7511 ± 1.57
NO_3	8565 ± 0.67	Nd	Nd

NA, not analyzed; Nd, not detected.

however, showed no trend while Sr, S, Y, Th, Rb, Pb and Nb showed limited concentration trends. Chemical analysis showed that the RO NA, not analyzed; Nd, not detected.

Quantification of the solid residues obtained after carbonation using water or brine for Run R31 was carried out to evaluate the effect of the liquid media used for fly ash dispersion on the relative amounts of the phases formed. Fig. 10 below shows the variation in the relative amounts of the mineral phases quantified in the solid residues recovered after water/brine carbonation.

The most important phenomena to note is that, the degree of calcite formation is higher in the brine carbonated residues compared to the water carbonated residues. The results confirm that brine contributes additional Ca^{2+} that enhances the degree of carbonation. Also evident is the fact that no lime was present in either the water or brine residues. The explanation for this would be that the lime in the brine reactions raised the brine pH for carbonation to occur while the lime in the water reactions hydrolyzed to the hydroxide form that later transformed to $CaCO_3$. Inboth cases the lime dissolved to release Ca^{2+} and hydroxyl ions which contributed to the increase in pH.

4. Conclusions

Brine impacted class F size fractionated fly ash has been carbonated under various conditions of pressure, temperature and L/S ratio. Chemical analysis of the size fractionated fly ash showed that the 20e150 mm fraction had the highest % CaO (9.3%) while the brine solutions applied in this study could be classified as $NaSO_4$ with major ions being Ca, K, Mg, Cl, SO_4 and Na. XRD confirmed the transformation of the CaO fraction in the un- carbonated FA to calcite in carbonated ash. Chittick tests and

quantitative XRD gave a reliable measure of correlation of the % $CaCO_3$ yield for the different experimental conditions applied. Statistical testing however showed Chititck tests to be a better estimator of the % $CaCO_3$ yield than XRD.
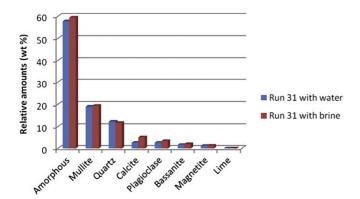

Fig. 10. Quantification of the phases present in the carbonation solid residues.

The study suggests a correlation between carbonation efficiency and size fraction of FA. Conversely, the XRD patterns, microscopic observations and chemical analyses showed clearly that the carbonation efficiency depends directly on the content of free lime onto FA. Here, the fast aqueous carbonation of 2 h reaction time was mainly related to spontaneous dissolution of free lime and initial dissolved Ca in brine, leading mainly to a homogenous nucleation of carbonates until an apparent equilibrium state or total consumption of free binary oxide (lime) in the slurry-CO_2 system.

The study has shown the feasibility of utilizing the two "waste products" i.e. FA and brine in the sequestration of CO_2. This would lower the treatment cost for RO effluents and contribute to brine stabilization in the form of mineral carbonates. Bearing in mind that some CO_2 point sources already produce pressurized and purified CO_2 emissions, these streams could be applied for carbonation at the source point as they do not require further purification or pressurization, thereby contributing towards cost reduction for CO_2 sequestration. Though utilization of waste FA and brine to reduce CO_2 emissions will not lead to significant carbon credits (calculated using tonnage of CO_2 sequestered) and hence carbon trading, these wastes are available in huge amounts and in close proximity to the emission sites hence transportation costs are lowered.

References

American Society for Testing and Materials, 1993. Standard Speciation for Fly Ash and Raw or Calcined Natural Pozzolans for Use As A Mineral Admixture in Portland Cement Concrete. ASTM, Philadelphia (PA).

Bachu, S., 2008. Prog. Energy Combustion Sci. 34, 254.

Baciocchi, R., Costa, G., Bartolomeo, E., Polettini, A., Pomi, R., 2009. Waste Manage. 29, 2994.

Davison, R.L., Natusch, D.F.S., Wallace, J.R., Evans Jr., C.A., 1974. Environ. Sci. Technol.8, 1107.

Druckenmiller, M.L., Maroto-Valer, M.M., 2005. Fuel Process. Technol. 86, 1599. Enders, M., 1996. Cem. Concr. Res. 26, 243.

Engelbrecht, A., Golding, A., Hietkamp, S., 2004. Council for Scientific and Industrial Research (CSIR), South Africa.

Fernandez, M.B., Li, X., Simons, S.J.R., Hills, C.D., Carey, P.J., 2004. Green Chem. 6, 428.

Huntzinger, D.N., Gierke, J.S., Sutter, L.L., Kawatra, K.S., Eisele, T.C., 2009. J. Hazard Mater.. doi:10.1016/j.jhazmat.2009.01.122.

Kaakinen, J.W., Jordan, R.M., Lawasani, M.H., West, R.E., 1975. Environ. Sci. Technol.
9, 862.

Klein, D.H., Andren, A.W., Carter, J.A., Emery, J.F., Feldman, C., Fulkerson, W., Lyon, W.S., Ogle, J.C., Talmi, Y., Van Hook, R.I., Bolt, N., 1995. Environ. Sci. Technol. 9, 973.

Kruger, R.A., 2003. Fuel 76, 777.

Kutchuko, B.G., Kim, A.G., 2006. Fuel 85, 2537.

Lin, L.K., 1989. Biometrics 45, 255.

Montes-Hernandez, G., Pérez-López, R., Renard, F., Nieto, J.M., Charlet, L., 2009. J. Hazard Mater. 161, 1347.

Mooketsi, I.O., Ginster, M., Matjie, H.R., Riedel, J.K., 2007. Presented at the World of Coal Ash (WOCA) conference, Kentucky, USA.

Perez-Lopez, R., Montes-Hernandez, G., Nieto, J.M., Renard, F., Charlet, L., 2008.Appl. Geochem. 23, 2292.

Petrik, L., Lewis, A.E., Hendry, B.A., 2007. Coaltech Report, South Africa. Pieterson, H.S., 1993. M.Sc. thesis, Delft University of Technology.

Randall, S., 2002. Sustainable energy watch report. Helio International, South Africa.

Sarkar, A., Rano, R., Udaybhanu, G., Basu, A.K., 2006. Fuel Process. Technol. 87, 259. Soong, Y., Fauth, D.L., Howard, B.H., Jones, J.R., Harrison, D.K., Goodman, A.L., Frommell, E.A., 2006. Energy Convers. Manage. 47, 1676.

Yadav, S.V., Prasad, M., Khan, J., Amritphale, S.S., Singh, M., Raju, C.B., 2009. J. Hazard. Mater.. doi:10.1016/j.jhazmat.2009.11.146.